The Interrelation among Network Structures, Molecular Transport of Solvent, and Creep Behaviors of TiB_2 Ceramic Containing Butyl Rubber Composites

Farid El-Tantawy

Department of Physics, Faculty of Science, Suez Canal University, Ismailia, Egypt

Received 1 September 2004; accepted 7 April 2005
DOI 10.1002/app.22424
Published online in Wiley InterScience (www.interscience.wiley.com).

ABSTRACT: Swelling of polymer composites in solvents has become one of the major problems in the use of polymer composites exposed to petroleum products. As a possible solution to the problem, this experimental study was conducted to examine the potential application of TiB_2 ceramic in butyl rubber (IIR) composites. The effect of TiB_2 content on the curing kinetics of IIR composites was studied using a torque rheometer technique. The effect of TiB_2 on the network structure was investigated in terms of the crosslinking density, interparticle distance between conducting particles, surface tension, glass transition temperature, degree of crystallinity, scanning electron microscopy, and X-ray analysis. Moreover, the effect of TiB_2 content on the molecular transport of solvent (kerosene) was examined by means of degree of swelling, solvent interaction parameters, volume fraction of rubber, interparticle distance after swelling, penetration rate of solvent, mean diffusion coefficient, cohesive energy density of polymer, standard entropy, standard enthalpy, and standard free energy of IIR composites. It was ascertained that with increasing TiB_2 content the degree of swelling shifts to a lower value. The main reason was interpreted as the introduction of good interface adhesion of TiB_2 with rubber matrix, which tends to block the diffusion of solvent molecules. The effect of TiB_2 content on hardness, tensile strength, Young's modules, and elongation at break is discussed. An apparent steady-state creep of butyl rubber IIR/TiB_2 composites is evident under different constant stresses at room temperature. The strain rate of steady-state creep showed a dependence on stress and TiB_2 volume fraction. The stress sensitivity parameter, viscosity coefficient, and activation volume for samples loaded with different content of TiB_2 were estimated. It is apparent that these new composites should be very useful for solvent permeation resistance at high TiB_2 loading level with good mechanical properties. © 2005 Wiley Periodicals, Inc. J Appl Polym Sci 98: 2226–2235, 2005

Key words: butyl rubber/TiB_2 composites; curing and network structure; swelling; mechanical properties

INTRODUCTION

The effects of fillers on the curing kinetics, network structure, and mechanical properties of elastomers are of great interest, primarily because fillers can be used very efficiently to enhance physicochemical properties.[1,2] Transition metal borides are a group of ceramic materials with outstanding and attractive properties for technological applications. Among these materials, TiB_2 has unusual chemical and physical properties such as high hardness, superior wear resistance, low density, high melting temperature, high modulus, high corrosion resistance, high electrical conductivity, and superconductivity at cryogenic temperatures. These outstanding features portray TiB_2 to be a good potential reinforcing candidate in polymer matrices. The interaction of polymeric materials with solvents is a serious problem from both the scientific and the practical view point.[3,4] The high degree of swelling is a common problem to all the bulk rubber composites. Two factors deteriorating the degree of swelling have been pointed out. One is a weak interface adhesion between filler and matrix, which acts as a channel for molecular transport of solvent into rubber matrix. Second is the crosslinking density of the rubber composites.[1] The dynamic properties of elastomers filled with structured fillers are influenced by different factors such as the type of filler, volume fraction of filler, and strain recovery.[5–9] Rubbers are viscoelastic in nature and their deformation properties are time and stress dependent. Creep describes the deformation of materials with time under constant stress and provides extremely important practical information on the reliability and lifetime of the materials.[9–12] Studies on dynamic creep are of paramount importance since most rubber compounds are subjected to some sort of dynamic loading. For these reasons it is important to take these into consideration as part of an overall effort to understand the creep behavior of butyl rubber (IIR)–TiB_2 composites. Several reviews show the effects of sulfur and carbon black contents as reinforc-

Correspondence to: F. El-Tantawy (faridtantawy@yahoo.com).

TABLE I
Composite Formulations Used in This Work

Ingredients	TB0	TB5	TB10	TB15	TB20	TB25
IIR	100	100	100	100	100	100
Stearic acid	2	2	2	2	2	2
ZnO	7	7	7	7	7	7
Glycerol	13	13	13	13	13	13
TMTD	1	1	1	1	1	1
PβN	1	1	1	1	1	1
TiB_2	0	5	10	15	20	25
Sulfur	2.5	2.5	2.5	2.5	2.5	2.5

ing fillers loaded into rubber matrix to improve physicochemical properties.[13–16] The possibilities offered by TiB_2 reinforcement of IIR composites have not yet been fully exploited. In the present work, a new type of composite material, viz., TiB_2 powder reinforced IIR composites, was developed. The influences of TiB_2 ceramic on curing network structure and molecular transport of solvent of IIR composites was investigated in detail. Some transport properties such as mean diffusion coefficient, penetration rate, cohesive energy of rubber, standard enthalpy, standard entropy, and standard free energy were evaluated as a function of TiB_2 content of IIR composites. Furthermore, the influence of TiB_2 content on the mechanical properties (hardness, Young's modules, tensile strength, elongation at break, and creep behavior) are also examined.

EXPERIMENTAL

Details of the formulation of the mixes are given in Table I. Butyl rubber (IIR) was manufactured by Transport and Engineering (rubber manufacturing) (TRENCO, Alexandria, Egypt) and had density 0.94 g/cm^3. Zinc oxide (ZnO), stearic acid, sulfur, tetramethyl thiuram disulfide (TMTD), and phenyl-β-naphthylamine (PβN) were of chemically pure grade. Glycerol was of pharmaceutical grade of specific gravity, 1.15. The titanium diboride (TiB_2) powder used in this study was supplied by Soekawa Chemical (Tokyo, Japan). According to the manufacturer's specification the specific surface area was 30 m^2/g and the particle size was 1–3 μm. The compounds were mixed in a two-roll mill of 170 mm diameter, working distance 300 mm, speed of slow roll 18 rpm, and gear ratio 1 : 4 by careful control of temperature, nip gap, and time of mixing. The IIR composites were left for 2 days before vulcanization in the normal air. The vulcanization process was carried out at 170 °C under a constant pressure of about 300 KN/m^2 for 30 min by molding in an electrically heated press. The curing parameters such as curing time (C_t) and scorch time (S_t) were determined from torque data obtained by a Monsanto rheometer (R-110). The complex dynamic shear moduli $G^* = G' + iG''$, were obtained with a rheometrics dynamic analyzer, Model RDA-III, Tokyo, Japan. The crosslinking density (CLD) was determined from the dynamic complex shear moduli at 60 °C using the relation[6,7]

$$\mathrm{CLD} = \frac{G'}{RT'} \tag{1}$$

where R is the universal gas constant and T is the absolute temperature.

Also, the glass transition temperature (T_g) was calculated from the dynamic complex shear moduli as the temperature where the loss modulus was at a maximum using the following equation:[5,6]

$$\tan\delta = \frac{G''}{G'}. \tag{2}$$

The surface tension (S_t) was measured by tension meter model (GPYP-A3, Tokyo, Japan). X-ray diffraction analysis (XRD) was performed by a diffractometer (Rigaku, Tokyo, Japan), equipped with a monochromater for CuKα ray, under the conditions of tube voltage, 20 KV; tube ampere:, 30 mA; and scanning speed, 0.5 °C/min. The degree of crystallinity (Z) was determined from differential scanning calorimetry (DSC) using the equation[2]

$$Z = \frac{\Delta H_f}{\Delta H_f^0 \omega_f}, \tag{3}$$

where ΔH_f is the apparent enthalpy (indicated in DSC thermographs as melting enthalpy per gram of composite) of fusion corresponding to the component, ΔH_f^0 is the enthalpy of fusion per gram of the component in its completely crystalline state, and ω_f is the weight fraction of the component. The microstructure was observed with a scanning electron microscope (SEM) and it was performed in a JEOL operated at 30 kV on surface samples without conducting coating. For mechanical measurements, the dumbbell-shape samples were prepared from the vulcanized rubber sheets with a different content of TiB_2 with dimensions 105 × 205 × 20 mm^3. Tensile strength (TS), Young's modules (YM), and elongation at break (EB) were determined using a tensile testing machine (ASTM D412). Tensile creep tests were then performed under constant stress at room temperature in an improved model creep machine similar to that described elsewhere.[14–16] The strain measurements were done with an accuracy of 1 × 10^{-5} m. The hardness (shore A) of each sample was measured according to the ASTM D2240 standard technique.[1] For measurement of swelling kinetics, the IIR composites were carefully cut into pieces about 10 × 10 × 10 mm^3 each. Initial mass was measured. The samples were immersed in kerosene solution and the change in mass with time was recorded for each 10 min.

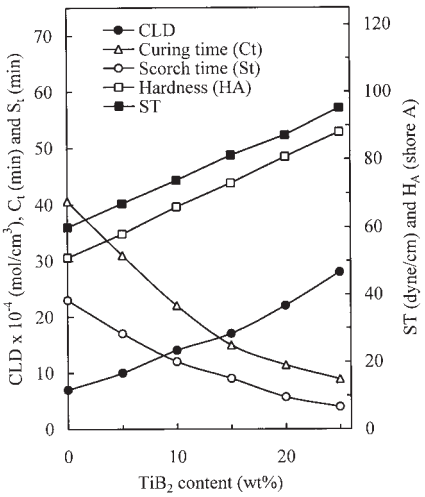

Figure 1 The variations of cure time (C_t), scorch time (S_t), surface tension (S_T), CLD, and hardness (H_A) as a function of TiB_2 content of IIR composites.

RESULTS AND DISCUSSION

The effects of TiB_2 on curing and network structure

The physical data of curing and network structure are needed for the fabrication of rubber composites industries. The variations of cure time (C_t), scorch time (S_t), surface tension (ST), CLD, and hardness (H_A) as a function of TiB_2 content are plotted in Figure 1, from which it is clear that the C_t and S_t of IIR composites decreases as the content of TiB_2 increases. The decrease in C_t and S_t may be due to an acceleration effect of TiB_2 particles on the vulcanization process (i.e., the TiB_2 particles increase the driving force of the curing kinetics into rubber matrix). This result suggests that during the curing process, the crosslinking density increases with increasing TiB_2 content in the rubber matrix. On the other hand, the CLD and S_t increase with increasing TiB_2 volume fraction in the composites. This might be due to the increase of interfacial adhesion and the decrease of the gap width between filler and matrix. The hardness increased from 51 to 88 (shore A) when its content increased from 0 to 25-wt %. This might be explained by the fact that the TiB_2 powder functions as a reinforcement for the IIR matrix, thereby stiffening the composite.[1–3]

The gap width between conductive particles (g) was calculated using the formula[1]

$$g = \left(\frac{\pi d^3 \rho_c}{6\varpi}\right)^{\frac{1}{3}} - 1, \qquad (4)$$

where ρ_c is the specific gravity of the composites, d is the TiB_2 particle diameter, and ϖ is the weight fraction of the filler, respectively.

The calculated values of g as a function of TiB_2 are plotted in Figure 2. As expected, the values of g decrease with increasing TiB_2 content in the composites. This confirms the previous conclusion of increases of the interface adhesion and crosslinking density with increasing TiB_2. To further evalute the effect of TiB_2 content on network structure, the glass transition temperature (T_g) and degree of crystallinity (Z) as a function of TiB_2 content are depicted in Figure 2. The increase of T_g with increasing TiB_2 content is probably related to the flexible structure and also the increase in crystallinity of the composites as supported by the degree of crystallinity in Figure 2. The results were further verified by X-ray diffractograms of the IIR composites in Figure 3. The XRD result for the green IIR showed clear partial crystallinity. The peaks located at 14.9, 36.3, and 36.3° refer to the IIR rubber. With the inclusion of TiB_2 into the rubber matrix, new peaks appear at 21.6, 23.8, and 34.7° related to TiB_2. The crystallinity increases with increasing TiB_2 content on the rubber matrix. The intensity of the peak for the TiB25 sample was approximately four times greater than that of the green sample (i.e., TiB0 sample).

Morphologies of IIR composites before and after swelling

The interface adhesion and crosslinking density in the rubber composites can be understood from the microstructure. Figure 4(a,b) shows SEMs for the unswollen prepared IIR composites for TB5 and TB25 samples, respectively. The micrographs show that with increasing TiB_2 content the TiB_2 particles become well-dispersed and interact better with the rubber matrix. These SEM observations are consistent with the net-

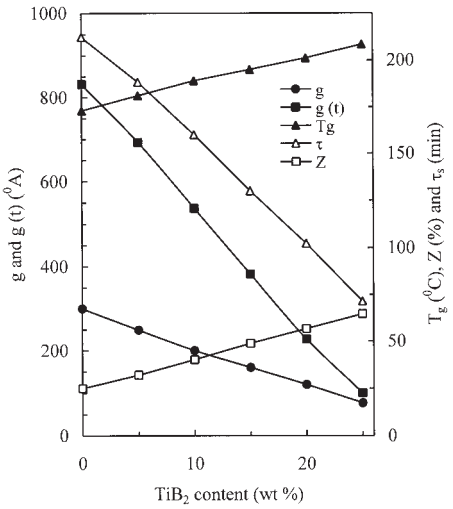

Figure 2 Degree of crystallinity, the gap width between conductive particles before and after swelling, glass transition temperature, and characteristic swelling time as a function of TiB2 content.

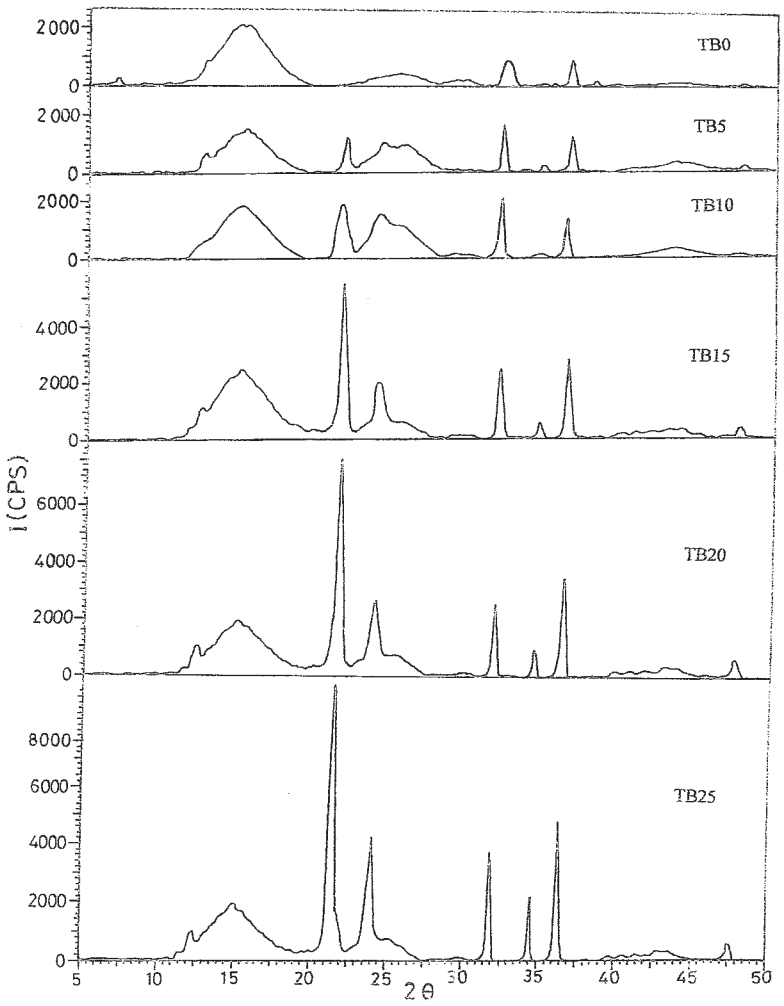

Figure 3 X-ray diffraction diagrams of IIR/TiB$_2$ composites.

work structure data described before and show the positive influence of TiB$_2$ on the mechanical properties of IIR composites. The morphologies of swollen TB5 and TB25 samples are shown in Figure 4(c,d). The micrograph of the TB5 sample clearly reveals the development of voids during swelling in the microstructure. There are voids and a dislocation network found for sample TB5 compared to TB25 sample after swelling in kerosene for 1 day. Therefore, it may be reasonable to assume that the gas barrier resistance increases with increasing TiB$_2$ in the composites. This indicates that the inclusion of TiB$_2$ into the rubber matrix increases the crystallinity and the quality of the network structure.

The effect of TiB$_2$ on molecular transport of kerosene

From the viewpoint of practice polymer composites, the degree of swelling in solvents is a most important and key property.[1–4] A low degree of swelling is necessary for applications not only for large-scale gas permeation resistance but also for high-efficiency electronic devices.[1] The degree of swelling (Q) was determined using the equation[1]

$$Q(\%) = \frac{m_i - m_0}{m_0} \times 100, \quad (5)$$

where m_0 and m_t are the masses of the specimen before and after swelling in solvent (kerosene), respectively.

Figure 5 shows the variation of Q with time (t) during swelling in kerosene of IIR composites. Clearly, there is a decrease in Q value with increasing volume fraction of TiB$_2$ in the IIR composites. This is attributed to the fact that at low TiB$_2$ content the separation distance among conductive phases increases and breaks down the network structure between particles, which leads to fast diffusion of the solvent molecules into the rubber matrix.[1] This may be the reason why a degree of swelling decreases with increasing TiB$_2$ in the matrix.

The $Q - t$ curve can be explained by an exponential growth function of the form[1,2]

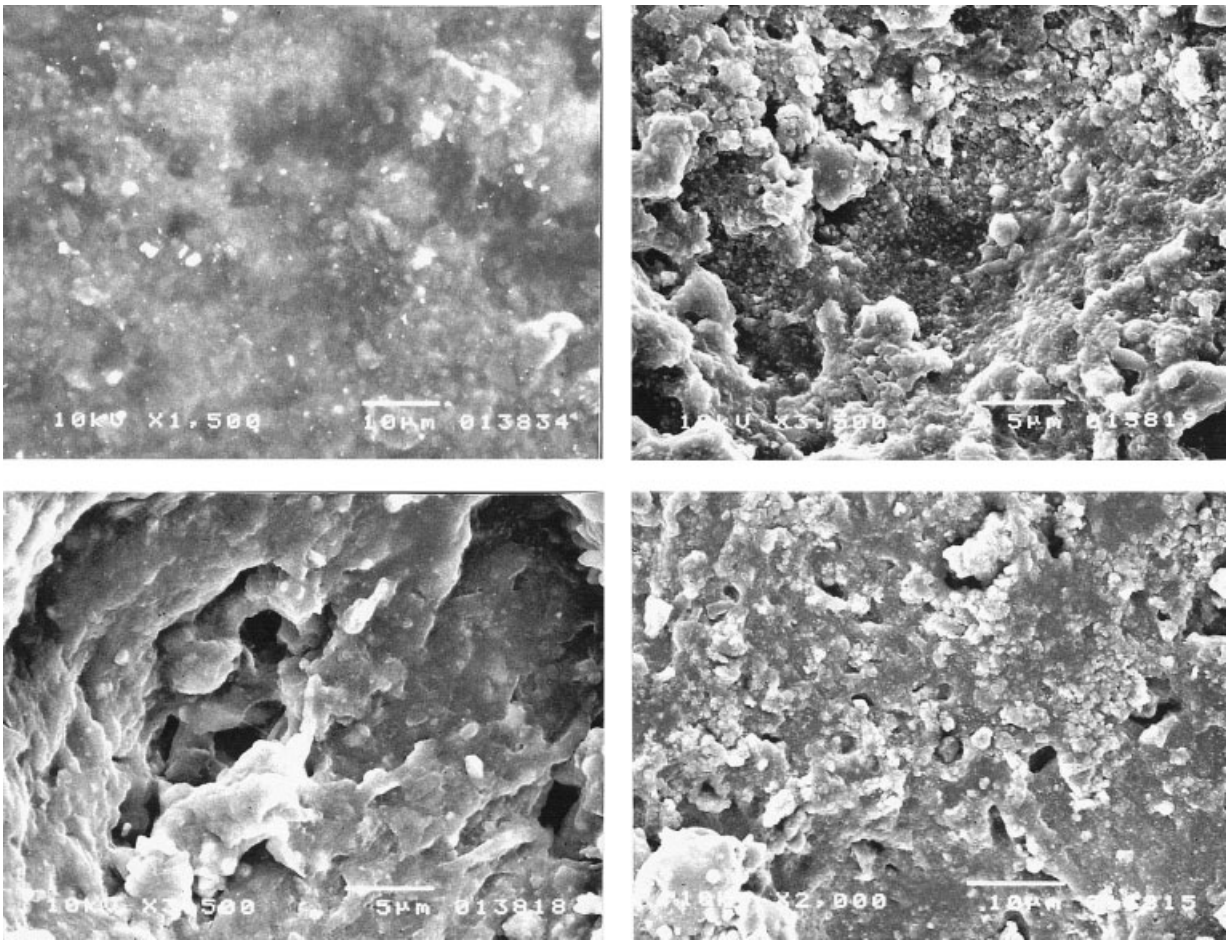

Figure 4 The scanning electron micrographs for (a) TB5, (b) TB25 before swelling, (C) TB5 after swelling, and (d) TB25 after swelling for IIR composites.

$$Q(t) = Q_m(1 - e^{-t/\tau_s}), \tag{6}$$

where Q_m is the degree of maximum swelling and τ_s is a characteristic swelling time constant that depends on TiB_2 content and is calculated at $t = \tau_s$.

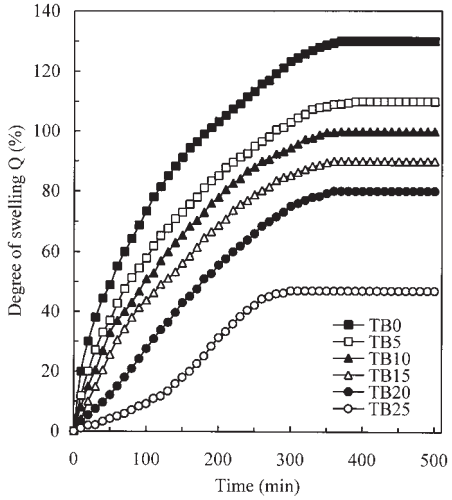

Figure 5 The variation of Q with time during swelling in kerosene of IIR composites.

The calculated values of τ_s as a function of TiB_2 content are plotted in Figure 2. It is seen that τ_s decreases as the volume fraction of TiB_2 increases. In other words, the rate of the specific change of swelling, $\frac{dQ}{dt} = \frac{1}{\tau_s}$, decreases with the increase in the content of TiB_2.[1–4] This implies that the stable structure and the interfacial adhesion among filler and matrix increase with increasing TiB_2 content in the rubber matrix as confirmed previously by SEM. This stable structure resists the diffusion of the kerosene molecules into the rubber matrix. Based on the above facts we think that the TiB_2 provides a barrier to prevent the diffusion of the solvent molecules into the rubber matrix. This fact could be also checked on the basis of the calculation of the interparticle distance during swelling in kerosene, $g(t)$, for all samples, which is given by[1,7]

$$g(t) = D\left(\left[1 + \frac{V_r}{V_c}\left(1 + \frac{\rho_r}{\rho_s}Q(t)\right)\right]^{\frac{1}{3}} - 1\right). \tag{7}$$

The calculated values of $g(t)$ after swelling in kerosene for 1 day as a function of TiB_2 are plotted in Figure 2.

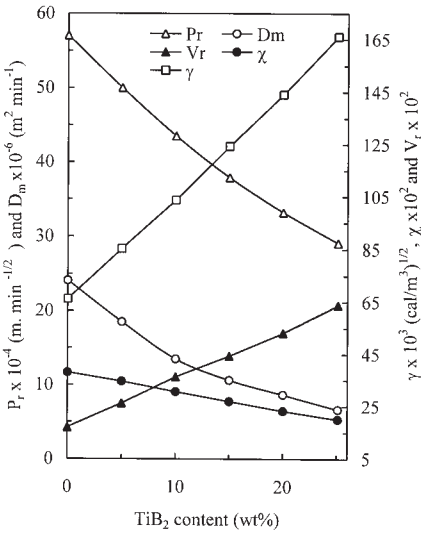

Figure 6 P_r and D_m, γ, χ, and V_r as a function of TiB_2 content of IIR composites.

The values of $g(t)$ decrease with increasing TiB_2 content in the composites and are greater compared to the value of g in Figure 2. This indicates that the TiB_2 particles provide a barrier to resist the diffusion of solvent molecules into the rubber matrix.

Transport properties of swollen composites

Knowledge of transport properties of swelling samples such as penetration rate, mean diffusion coefficient, and cohesive energy density, standard entropy, standard enthalpy, and standard free energy are necessary for practical application such as solvent resistance materials. The penetration rate (P_r) of kerosene during swelling is given by[1,15]

$$P_r = \left(\frac{h}{2M_e}\right)\left(\frac{M_t}{\sqrt{f}}\right), \tag{8}$$

where M_e and M_t are the weight uptakes of the solvent at equilibrium and swollen polymer at time t, respectively, and f is the polymer thickness.

The relation between P_r and the mean diffusion coefficient (D_m) of solvent is given by[1,4]

$$D_m = \frac{\pi P_r^2}{4}. \tag{9}$$

Figure 6 shows the P_r and D_m as a function of TiB_2 content of IIR composites. It is seen that both P_r and D_m decrease with increasing TiB_2 content in the composites. This supports the thesis that the inclusion of TiB_2 into the rubber matrix increases the chain connectivity and solvent permeation resistance.

The cohesive energy density (γ) of polymer is given by[1,4]

$$(\gamma_s - \gamma)^2 = \frac{\chi RT}{V_1}, \tag{10}$$

where γ_s is the cohesive energy density of kerosene and is about 7.66 $(cal/cm^3)^{0.5}$, V_1 is the molar volume of the kerosene and is about 180 (cm^3/mol), R is the universal gas constant, and χ is the polymer–solvent interaction parameter given by[1]

$$\chi = 0.431 - 0.311V_r + 0.036V_r^2. \tag{11}$$

The volume fraction of rubber (V_r) was determined using the equilibrium swelling method and is given by[1]

$$V_r = \frac{\rho_s M_r}{\rho_s M_r + \rho_r M_s}, \tag{12}$$

where ρ_s and ρ_r are the solvent and rubber density, respectively, and M_r and M_s are the weights of dry rubber and adsorbed solvent, respectively.

The relationship among γ, χ, and V_r versus TiB_2 content is plotted in Figure 6. It is clear that χ decreases while γ and V_r increase as TiB_2 content increases in the matrix. The decrease in χ and the increase in γ and V_r are due to the decreasing volume fraction of rubber and intermolecular distance in the composites with increased TiB_2 loading.
The standard entropy (ΔS) is given by[1]

$$\Delta S = -R\left[\ln(1 - V_r) + V_r + \frac{\rho_r V_1}{M_c(V_r^{\frac{1}{3}} - 0.5V_r)}\right], \tag{13}$$

where M_c is the molecular weight between physical crosslinks and is calculated using the equation

$$M_c = -V_r\rho_r\frac{\left(V_r^{\frac{1}{3}} - \frac{V_r}{2}\right)}{[\ln(1 - V_r) + V_r + \chi V_r^2]}. \tag{14}$$

The standard free energy (ΔG) and the standard enthalpy (ΔH) are given by[1]

$$\Delta G = RT[\ln(1 - V_r) + V_r + \chi V_r^2] \tag{15}$$

$$\Delta H = \Delta G + T\Delta S. \tag{16}$$

The variations of ΔS, ΔG, and ΔH as a function of TiB_2 content are plotted in Figure 7 It is clearly seen that the ΔS, ΔG, and ΔH increase with increasing TiB_2 content in the rubber matrix. This is ascribed to the increase of interface adhesion and crosslinking density with increasing TiB_2 loading level in the rubber matrix. It is interesting to note that the enthalpy values are positive and free energy is negative. This reflects that the

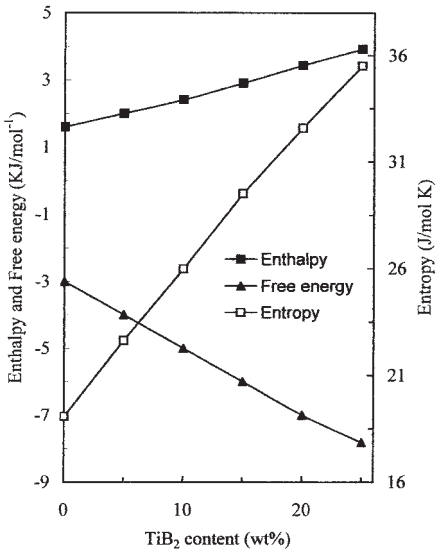

Figure 7 Enthalpy, entropy, and free energy versus TiB_2 content of IIR composites.

sorption mechanism of solvent in IIR composites is an endothermic process and proceeds through creating new paths and/or holes in the rubber matrix.

Features of creep behaviors

The creep curves obtained for samples containing different concentrations of TiB_2 are shown in Figure 8(a–f). The samples were investigated at room temperature under constant applied stresses ranging from 3.13 to 8.60 MPa. The trend in the creep curves at all the levels of applied stresses suggests a rapid transition from a short primary creep regime to a steady-state creep regime. This shows that the creep behavior of the samples is similar to that exhibited by pure metals and alloys.[14–16] Since the stress and temperature are constants, the variation in creep rates ($\varepsilon^{\bullet}$) suggests a basic change in the internal structure of the composite during time. Figure 8(a–f) also shows that the samples with higher TiB_2 content exhibited higher creep resistance and lower total elongation. According to the aforementioned results, the strengthening effect of TiB_2 was significant, since the creep rate and creep strain decreased as the TiB_2 increased. Again, at higher stresses, the creep curves clearly show slight separation toward the high strains, and then strain failure is observed. This is thought to be due to an increase in the high local stresses concentrations that occur from progressive rupture of individual chain segment within the rubber matrix and/or radial stresses at the TiB_2 butyl rubber interface.[1–3] The steady-state creep rate ($\dot{\varepsilon}_{st}$) increases with increasing applied stress (σ) while it decreases with increasing TiB_2 content. The noticeable dependence of strain rate on the applied stress is simply associated with the onset of significant plastic flow, and on a molecular level it is anticipated that it may be associated with interaction sliding and chain segmental motion. In this context, it is to be noted that when a stress is applied over a chain segment, the free energy increases, which causes enhancement of the flow mobility of chain segments.[12,13] On the other hand, the decrease in $\dot{\varepsilon}_{st}$ values is connected with filler–matrix interaction, with the chemical interaction leading to an increase in the crosslinking density with increasing filler content, which leads to hardening of the samples. An additional contribution resulting from the presence of TiB_2 among the formed aggregates between polymeric chains appears to play an important role in governing the creep behavior, which leads to some loss of chain mobility and a degree of immobilization.[6] It is clear that one of the major limitations to attaining large strains period to failure is the presence of TiB_2 and its large contribution in the creep process. To confirm the above idea, the TS, YM, and EB are depicted in Figure 9. It is clear that the TS and YM increase with increasing TiB_2 content in the composites. On the other hand, EB decreases with increasing TiB_2 content in the composites. This is attributed to the fact that with increasing the TiB_2 content, the crosslinking extent increased and the entanglement of the networks also increased, so the pennetration of TiB_2 among macromolecular chains can be prevented. Thus, the TS and YM were enhanced while EB decreased.

Stress dependence of steady state creep rate

The stress dependence of the steady-state creep rate ($\dot{\varepsilon}_{st}$) follows the power law,

$$\dot{\varepsilon}_{st} = A\exp\left(\frac{-(E_a - V_a\sigma)}{KT}\right), \qquad (17)$$

where A is a constant, σ is the applied stress, E_a is the activation energy of the flow process, and V_a is the activation volume.

Equation (17) was used for the estimation of the V_a by plotting $\ln\dot{\varepsilon}_{st}$ versus σ at constant testing temperature. In the steady-state creep, the apparent activation volume (V_a) was found to decrease markedly with increasing applied stress for all tested samples, as seen in Figure 10. A significant decrease in the magnitude of V_a occurs with increasing TiB_2 volume fraction. It is reasonable to consider this behavior as being due to the effect of crosslinks. The stress and concentration dependence of apparent activation volume could be simply related to the degree of crosslink density, where the nature of the crosslinks may be to immobilize the motion of molecular segments due to the formation of aggregates. The sensitivity parameter (n) is calculated by the equation[12]

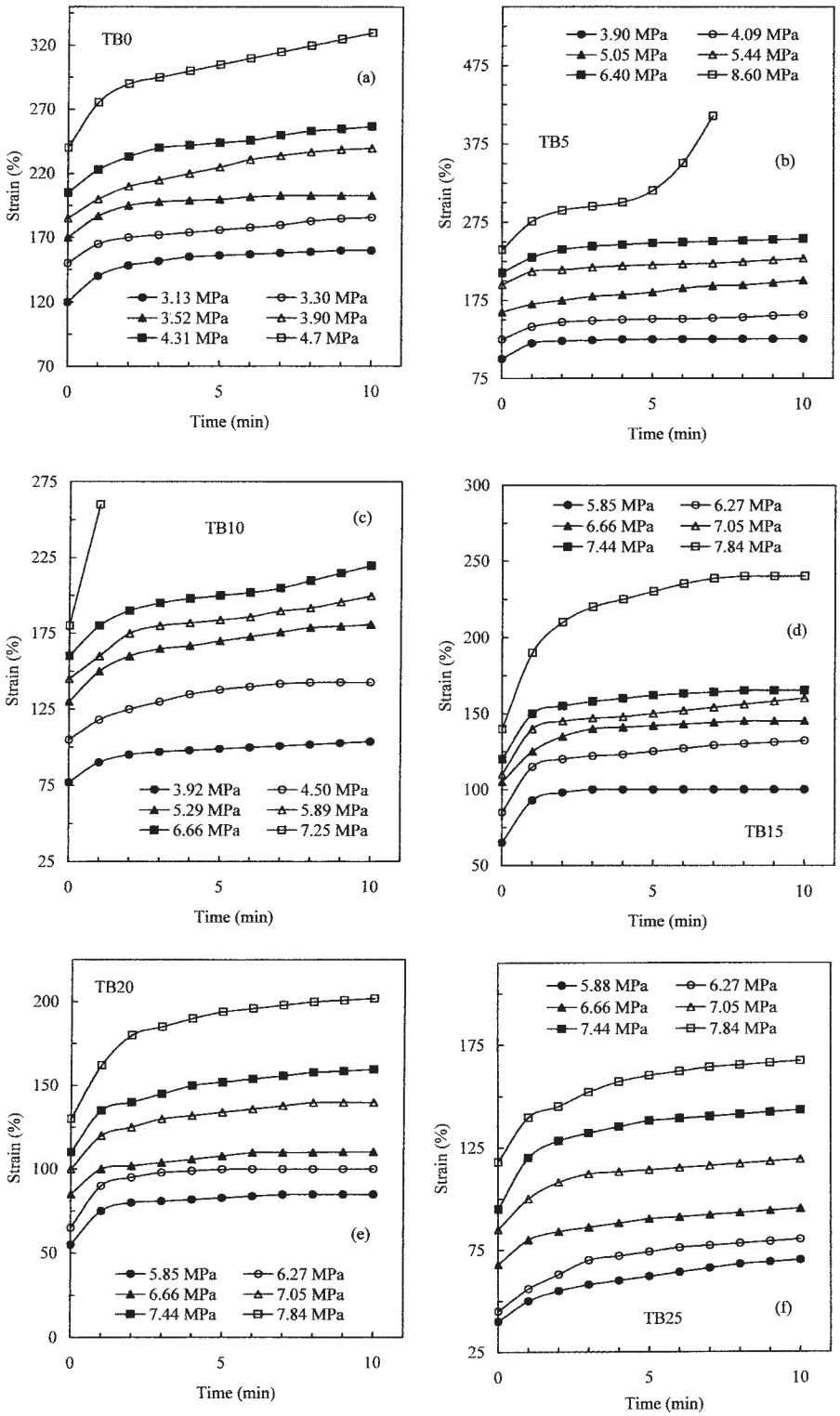

Figure 8 The strain against time curve for all tested samples containing different content of TiB_2 at room temperature and different applied stress for IIR composites.

$$n = \left(\frac{\delta \ln \varepsilon_{st}^{\bullet}}{\delta \ln \sigma}\right)_T. \tag{18}$$

The calculated values of (n) are plotted versus TiB_2 contents in Figure 11. It can be seen that n decreases from 2.90 to 1.50 as TiB_2 increases in the composites. This means that the rubber composites lost sensitivity toward the applied stress and become unable to relax sufficiently. We suggest that the above values of the stress sensitivity parameter can be explained by the

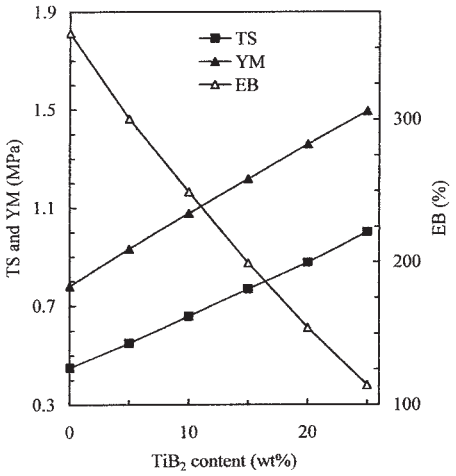

Figure 9 Tensile stress, Young's modulus, and elongation at break versus TiB_2 content of IIR composites.

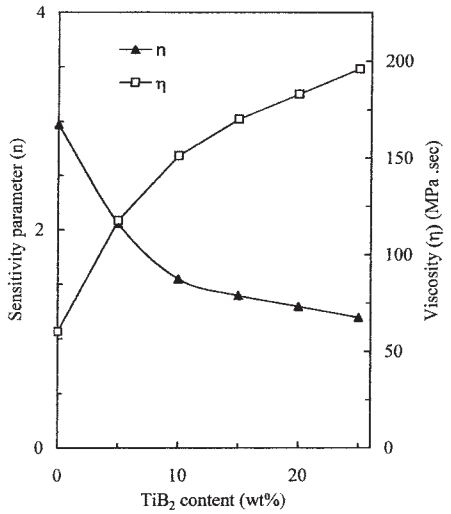

Figure 11 Viscosity and sensitivity parameter versus TiB_2 content of IIR composites.

viscous motion of the chain segments due to the presence of TiB_2 and its interaction with rubber chains: the n values decrease as the viscosity increases. Thus, it was possible to follow the variation of the viscosity coefficient (ç) with the concentration of TiB_2 in the samples. The viscosity (ç) was measured from creep curves using the relation[1]

$$\eta = \frac{\sigma}{\varepsilon_{st}^{\bullet}}. \tag{19}$$

The variation of viscosity against TiB_2 content is plotted in Figure 11. The increase of viscosity with TiB_2 content can be explained in that the TiB_2 may provide an additional mechanism by which the strain energy is dissipated. The greater the dissipation, the greater the strength. The strength may be raised due to the formation of aggregates, which impede the movement of chain segments and lead to increasing matrix viscosity.

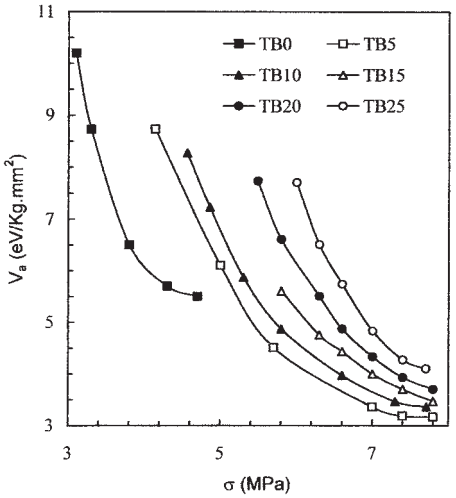

Figure 10 Activation volume against applied stress for IIR composites.

CONCLUSIONS

The following conclusions can be drawn from our work:

1. The curing and network structure of the IIR/TiB_2 composites is strongly dependent on concentration of TiB_2 particles. The TiB_2 content accelerates the driving force of the curing process and increases the crosslinking density and is well adhered with butyl rubber.
2. The viscosity and surface tension increase with increasing TiB_2 content. This indicates that the TiB_2 can act as a network former within the rubber matrix.
3. The degree of swelling of solvent (kerosene) in IIR composites decreases as the concentration of TiB_2 increases. The composites exhibit good permeation resistance in kerosene with increasing TiB_2 content in the rubber matrix.
4. The mean diffusion coefficient and penetration rate decrease while cohesive energy density increases with increasing TiB_2 content in the rubber matrix. The sorption mechanism of solvent in IIR composites is controlled by an endothermic process.
5. The inclusion of TiB_2 particles in butyl rubber matrix improves high creep resistance when samples are subjected to similar stresses and increased TiB_2 volume fraction increases creep resistance, tensile strength, and Young's modulus.

References

1. El-Tantawy, F. Polym Degrad Stabil 2001, 73, 289.
2. El-Tantawy, F.; Abdel Kader, K.; Kaneko, F.; Song, Y. K. Eur Polym J 2004, 40, 415.

3. El-Tantawy, F.; Dishovsky, N. J Appl Polym Sci 2004, 91, 2756.
4. Suwanpratee, J.; Tanner, B. K. E.; Turner, S.; Bonfield, W. J Mater Sci 1995, 6, 804.
5. Khaled, M. A.; Hasaan, E. A.; Elwy, A.; Metwally, E. E. Mater Lett 1994, 19, 325.
6. Gwaily, S. E.; Badawy, M. M.; Hassan, H. H.; Madani, M. Polym Test 2003, 22, 3.
7. Raj, S. V. J Mater Sci 1999, 24, 3196.
8. Faez, R.; Martin, I. M.; De Paoli, M.; Rezede, M. C. J Appl Polym Sci 2002, 83, 1568.
9. Ismail, H.; Shuhelmy, S.; Edyham, M. R. Eur Polym J 2002, 38, 39.
10. Dutta, N. K.; Tripathy, D. K. J Appl Polym Sci 1992, 44, 1635.
11. Hassan, H. H.; Nasr, G. M. J Macromol Sci Chem 1982, 18, 535.
12. Hamza, S. S.; Osman, H. Polym Bull 1985, 12, 209.
13. Mahmoud, S. A.; Semary, M. A.; Farid, Z. M.; Elnaquib, N. A. Phys Stat Sol 1991, 127, 111.
14. El- Daly, A. A.; Abdel Daiem, A. M.; Yosef, M. Mater Chem Phys 2001, 71, 111.
15. El- Daly, A. A.; Abdel Daiem, A. M.; Yosef, M. Mater Chem Phys 2002, 74, 48.
16. El- Daly, A. A.; Abdel Daiem, A. M.; Abdel Rahman, A. N.; Mohamed, S. M. Mater Chem Phys 2004, 83, 96.